Spatial Correlations of a 3-D Non-Stationary MIMO Channel Model With 3-D Antenna Arrays and 3-D Arbitrary Trajectories

Qiuming Zhu, *Member, IEEE*, Ying Yang, Cheng-Xiang Wang, *Fellow, IEEE*, Yi Tan, Jian Sun, *Member, IEEE*, Xiaomin Chen, and Weizhi Zhong

***Abstract*—By considering the 3-D antenna arrays and 3-D arbitrary trajectories of a mobile station, a generic non-stationary geometry-based stochastic model for multiple-input multiple-output channels is proposed. Under 3-D non-isotropic von Mises-Fisher scattering scenarios, the theoretical and approximate expressions of time-variant spatial correlation function (SCF) are also derived and analyzed. Simulation results show that the SCFs of proposed model match well with the ones of existing models for the special cases of 1-D linear and 2-D curve trajectories. In addition, the derived theoretical SCFs also have good agreements with simulated and measured results.**

***Index Terms*—Non-stationary MIMO channels, geometry-based stochastic model (GBSM), spatial correlation (SC), von Mises-Fisher (VMF), arbitrary trajectories.**

I. Introduction

MULTIPLE-INPUT multiple-output (MIMO) technologies have drawn attention for their ability to increase spectral efficiency and system capacity significantly [1]. Meanwhile, despite difficulty and high price in realization, the three dimensional (3D) antenna array is a promising solution to improve directional performance of MIMO systems. However, insufficient antenna spacing or lack of scattering would reduce these benefits due to increased spatial correlation (SC). Therefore, the exploitation of SC is vital for design, optimization, and performance evaluation of wireless MIMO communication systems. Especially, the closed-form expressions of spatial correlation functions (SCFs) are essential to derive the theoretical results of system performance [2], [3], i.e., capacity, energy efficiency, and bit error rate (BER).

Most of SCFs in [3] and [4] were investigated for the stationary MIMO channels with wide-sense stationarity (WSS) assumption. Measurement campaigns have proved that the WSS assumption is only valid for short time intervals and the non-stationarity should be considered [1]. Recently, a few 3D non-stationary MIMO channel models have been presented in [5]–[10]. However, the models in [5]–[8] only considered 3D scattering environments but assumed the mobile station (MS) moving with a constant velocity (or 1D linear trajectory). Bian *et al.* [9] and Borhani *et al.* [10] took the velocity variations of MS into account, but they only considered 2D curve trajectories on the azimuth plane. For simplicity purpose, the MS in [5]–[10] was configured with a uniform linear array or 2D antenna array. In addition, the corresponding SCFs were usually analyzed numerically due to complex mathematical derivations. This letter aims to fill these research gaps. Overall, the major contributions and novelties of this letter are summarized as follows:

1) This letter develops a new generic 3D non-stationary geometry-based stochastic model (GBSM) for MIMO channels. The proposed GBSM allows for 3D scattering environments, 3D antenna arrays, and 3D arbitrary trajectories of the MS, which makes it more realistic and suitable for a wide variety of communication scenarios.

2) We derive the theoretical and approximate expressions of time-variant SCFs for our proposed GBSM under 3D von Mises-Fisher (VMF) scattering scenarios which are flexible and allow the dependence between azimuth angles and elevation angles.

The remainder of this letter is organized as follows. Section II gives a new generic 3D non-stationary GBSM. In Section III, the theoretical and approximate expressions of SCF for our proposed GBSM under 3D VMF scattering scenarios are derived. In Section IV, the SCFs of proposed model for three typical trajectories are simulated and validated. Finally, some conclusions are given in Section V.

Manuscript received July 27, 2018; revised September 4, 2018 and October 13, 2018; accepted October 17, 2018. Date of publication October 26, 2018; date of current version April 9, 2019. This work was supported by EU H2020 ITN 5G Wireless Project under Grant 641985, in part by EU H2020 RISE TESTBED Project under Grant 734325, in part by EPSRC TOUCAN Project under Grant EP/L020009/1, in part by the National Key Scientific Instrument and Equipment Development Project under Grant 2013YQ200607, in part by NSF of China under Grant 61631020 and Grant 61827801, in part by the Open Foundation for Graduate Innovation of NUAA under Grant KFJJ20170405, in part by the Taishan Scholar Program of Shandong Province, and in part by Fundamental Research Funds of Shandong University under Grant 2017JC009. The associate editor coordinating the review of this paper and approving it for publication was V. Raghavan. *(Corresponding author: Cheng-Xiang Wang.)*

Q. Zhu is with the Key Laboratory of Dynamic Cognitive System of Electromagnetic Spectrum Space, College of Electronic and Information Engineering, Nanjing University of Aeronautics and Astronautics, Nanjing 211106, China, and also with the Institute of Sensors, Signals and Systems, School of Engineering and Physical Sciences, Heriot-Watt University, Edinburgh EH14 4AS, U.K. (e-mail: zhuqiuming@nuaa.edu.cn).

Y. Yang, X. Chen, and W. Zhong are with the Key Laboratory of Dynamic Cognitive System of Electromagnetic Spectrum Space, College of Electronic and Information Engineering, Nanjing University of Aeronautics and Astronautics, Nanjing 211106, China (e-mail: yingy@nuaa.edu.cn; chenxm402@nuaa.edu.cn; zhongwz@nuaa.edu.cn).

C.-X. Wang is with the National Mobile Communications Research Laboratory, School of Information Science and Engineering, Southeast University, Nanjing 210096, China, and also with the Institute of Sensors, Signals and Systems, School of Engineering and Physical Sciences, Heriot-Watt University, Edinburgh EH14 4AS, U.K. (e-mail: chxwang@seu.edu.cn).

Y. Tan is with the Institute of Sensors, Signals and Systems, School of Engineering and Physical Sciences, Heriot-Watt University, Edinburgh EH14 4AS, U.K. (e-mail: yi.tan@hw.ac.uk).

J. Sun is with the Shandong Provincial Key Laboratory of Wireless Communication Technologies, School of Information Science and Engineering, Shandong University, Qingdao 266237, China (e-mail: sunjian@sdu.edu.cn).

Digital Object Identifier 10.1109/LWC.2018.2878210

II. The Generic 3D Non-Stationary GBSM

Let us consider a non-stationary MIMO channel under 3D scattering environments between a base station (BS) equipped with *S* antennas and a MS equipped with *U* antennas. There are two coordinate systems, i.e., the BS coordinate system $\tilde{x}\tilde{y}\tilde{z}$ and the MS coordinate system *xyz*. In the BS coordinate system, $\mathbf{d}_s^{\mathrm{BS}} = [d_s^{\mathrm{BS},\tilde{x}}, d_s^{\mathrm{BS},\tilde{y}}, d_s^{\mathrm{BS},\tilde{z}}]^{\mathrm{T}}$ denotes the 3D location of BS antenna element *s*, while $\phi_{n,m}^{\mathrm{BS}}(t)$ and $\theta_{n,m}^{\mathrm{BS}}(t)$ represent the azimuth angles of departure (AAoDs) and elevation angles of departure (EAoDs) of the *m*th ray within the *n*th path, respectively. Note that the MS coordinate origin is the center of MS and *x* axis is the initial movement direction of MS. The time-variant velocity vector of MS is denoted by $\mathbf{v}^{\mathrm{MS}}(t)$. Consequently, the 3D location of MS antenna element *u* in the MS coordinate system should be time-variant and is denoted as $\mathbf{d}_u^{\mathrm{MS}}(t) = [d_u^{\mathrm{MS},x}(t), d_u^{\mathrm{MS},y}(t), d_u^{\mathrm{MS},z}(t)]^{\mathrm{T}}$. The azimuth angles of arrival (AAoAs) and the elevation angles of arrival (EAoAs) of the *m*th ray within the *n*th path are denoted by $\phi_{n,m}^{\mathrm{MS}}(t)$ and $\theta_{n,m}^{\mathrm{MS}}(t)$, respectively. In this letter, the twin-cluster approach in [11] is adopted. The first and last clusters denoted by A_n and Z_n, respectively, are considered having random velocities denoted as $\mathbf{v}^{\mathrm{A}_n}(t)$ and $\mathbf{v}^{\mathrm{Z}_n}(t)$, respectively, while $v^{\mathrm{A}_n/\mathrm{Z}_n}$, $\phi^{\mathrm{A}_n/\mathrm{Z}_n}$, and $\theta^{\mathrm{A}_n/\mathrm{Z}_n}$ denote their amplitudes, azimuth, and elevation angles, respectively. The rest of clusters are abstracted by several virtual links. Note that the mean angles of AAoDs and EAoDs are denoted by $\bar{\phi}_n^{\mathrm{BS}}(t)$ and $\bar{\theta}_n^{\mathrm{BS}}(t)$, respectively, while the mean angles of AAoAs and EAoAs are denoted by $\bar{\phi}_n^{\mathrm{MS}}(t)$ and $\bar{\theta}_n^{\mathrm{MS}}(t)$.

The small-scale fading channel between the BS and MS can be expressed by an $U \times S$ complex matrix. Each element $h_{u,s}(t,\tau)$ denotes the complex channel impulse response (CIR) between the *s*th BS antenna and the *u*th MS antenna, and it can be modeled as [8]

$$h_{u,s}(t,\tau) = \sum_{n=1}^{N(t)} \sqrt{P_n(t)}\tilde{h}_{u,s,n}(t)\delta(\tau - \tau_n(t)) \tag{1}$$

where $N(t)$ multiple paths are characterized by a path delay $\tau_n(t)$, path power $P_n(t)$, and channel coefficient $\tilde{h}_{u,s,n}(t)$.

It should be mentioned that the channel parameters of (1) such as $N(t)$, $P_n(t)$, and $\tau_n(t)$ are time-invariant in WINNER+ model. Here, they are upgraded to be time-variant to capture the non-stationarity of real channels. Moreover, our previous 3D non-stationary GBSMs in [8] as well as other existing GBSMs only considered 1D or 2D trajectories and antenna arrays of the MS. In order to take 3D arbitrary trajectories and antenna arrays into account, this letter models $\tilde{h}_{u,s,n}(t)$ as

$$\tilde{h}_{u,s,n}(t) = \lim_{M\to\infty} \sqrt{\frac{1}{M}} \sum_{m=1}^{M} \mathrm{e}^{\mathrm{j}(\Phi_{n,m}^{\mathrm{D}}(t)+\Phi_{n,m}^{\mathrm{L}}(t)+\Phi_{n,m}^{\mathrm{I}})} \tag{2}$$

where *M* denotes the number of rays, and $\Phi_{n,m}^{\mathrm{I}}$ is a random initial phase uniformly distributed over $[0, 2\pi)$. In (2), $\Phi_{n,m}^{\mathrm{D}}(t)$ and $\Phi_{n,m}^{\mathrm{L}}(t)$ denote the time-variant phases caused by Doppler frequency variations and antenna location variations, respectively, and they can be further modeled as [12]

$$\Phi_{n,m}^{\mathrm{D}}(t) = \int_0^t \mathrm{k}\Big(\mathbf{v}^{\mathrm{MS}}(t') - \mathbf{v}^{\mathrm{Z}_n}(t')\Big)\tilde{\mathbf{s}}_{n,m}^{\mathrm{MS}}(t')\mathrm{d}t' \tag{3}$$

and

$$\Phi_{n,m}^{\mathrm{L}}(t) = \mathrm{k}((\tilde{\mathbf{s}}_{n,m}^{\mathrm{MS}}(t))^{\mathrm{T}} \cdot \mathbf{R}_{\mathbf{v}}(t) \cdot \mathbf{d}_u^{\mathrm{MS},t_0} + (\tilde{\mathbf{s}}_{n,m}^{\mathrm{BS}}(t))^{\mathrm{T}} \cdot \mathbf{d}_s^{\mathrm{BS}}) \tag{4}$$

where k is the wave number, $\mathbf{d}_u^{\mathrm{MS},t_0}$ denotes the initial 3D location of the *u*th MS antenna, $\tilde{\mathbf{s}}_{n,m}^{\mathrm{MS}}(t)$ and $\tilde{\mathbf{s}}_{n,m}^{\mathrm{BS}}(t)$ are the equivalent spherical unit vectors of the *m*th ray within the *n*th path of arrival and departure signals, respectively, and can be expressed as

$$\tilde{\mathbf{s}}(\phi_{n,m}^{\mathrm{BS/MS}}(t), \theta_{n,m}^{\mathrm{BS/MS}}(t)) = \begin{bmatrix} \cos(\theta_{n,m}^{\mathrm{BS/MS}}(t))\cos(\phi_{n,m}^{\mathrm{BS/MS}}(t)) \\ \cos(\theta_{n,m}^{\mathrm{BS/MS}}(t))\sin(\phi_{n,m}^{\mathrm{BS/MS}}(t)) \\ \sin(\theta_{n,m}^{\mathrm{BS/MS}}(t)) \end{bmatrix}. \tag{5}$$

Note that the time-variant rotation matrix $\mathbf{R}_{\mathbf{V}}(t)$ in (4) takes the effect of 3D arbitrary trajectories into account and can be calculated by

$$\mathbf{R}_{\mathbf{V}}(t) = \begin{bmatrix} \cos\theta_{\mathbf{V}}(t)\cos\phi_{\mathbf{V}}(t) & -\sin\phi_{\mathbf{V}}(t) & -\sin\theta_{\mathbf{V}}(t)\cos\phi_{\mathbf{V}}(t) \\ \cos\theta_{\mathbf{V}}(t)\sin\phi_{\mathbf{V}}(t) & \cos\phi_{\mathbf{V}}(t) & -\sin\theta_{\mathbf{V}}(t)\sin\phi_{\mathbf{V}}(t) \\ \sin\theta_{\mathbf{V}}(t) & 0 & \cos\theta_{\mathbf{V}}(t) \end{bmatrix} \tag{6}$$

where $\phi_{\mathbf{V}}(t)$ and $\theta_{\mathbf{V}}(t)$ denote the azimuth and elevation angles of $\mathbf{v}^{\mathrm{MS}}(t)$, respectively.

III. The SCFs Under 3D VMF Scattering Scenarios

A. Theoretical SCFs of the Generic 3D Non-Stationary GBSM

The normalized time-variant SCF of the *n*th path between two different pairs of antennas can be defined as

$$\rho_{u_1,s_1,n}^{u_2,s_2,n}(t;\Delta\mathbf{d}) = \mathrm{E}\Big\{\tilde{h}_{u_1,s_1,n}(t)\tilde{h}_{u_2,s_2,n}^{*}(t)\Big\}. \tag{7}$$

Since clusters A_n and Z_n are usually considered independent, the normalized SCF can be rewritten as

$$\rho_{u_1,s_1,n}^{u_2,s_2,n}(t;\Delta\mathbf{d}) = \rho_{s_1,s_2,n}^{\mathrm{BS}}(t;\Delta\mathbf{d}^{\mathrm{BS}}) \cdot \rho_{u_1,u_2,n}^{\mathrm{MS}}(t;\Delta\mathbf{d}^{\mathrm{MS}}) \tag{8}$$

where $\rho_{s_1,s_2,n}^{\mathrm{BS}}(t;\Delta\mathbf{d}^{\mathrm{BS}})$ and $\rho_{u_1,u_2,n}^{\mathrm{MS}}(t;\Delta\mathbf{d}^{\mathrm{MS}})$ denote normalized SCFs at the BS and the MS, respectively. By substituting (2)–(4) into (7), they can be calculated as

$$\begin{aligned}\rho_{s_1,s_2,n}^{\mathrm{BS}}(t;\Delta\mathbf{d}^{\mathrm{BS}}) = \int_{-\pi}^{\pi}\int_{-\pi}^{\pi} & \mathrm{e}^{\mathrm{jk}(\tilde{\mathbf{s}}_n^{\mathrm{BS}}(t))^{\mathrm{T}}\cdot\Delta\mathbf{d}^{\mathrm{BS}}} \\ & \times p_{\phi_{n,m}^{\mathrm{BS}}(t),\theta_{n,m}^{\mathrm{BS}}(t)}(\phi_n^{\mathrm{BS}}(t),\theta_n^{\mathrm{BS}}(t))\mathrm{d}\phi_n^{\mathrm{BS}}\mathrm{d}\theta_n^{\mathrm{BS}}\end{aligned} \tag{9}$$

$$\begin{aligned}\rho_{u_1,u_2,n}^{\mathrm{MS}}(t;\Delta\mathbf{d}^{\mathrm{MS}}) = \int_{-\pi}^{\pi}\int_{-\pi}^{\pi} & \mathrm{e}^{\mathrm{jk}(\tilde{\mathbf{s}}_n^{\mathrm{MS}}(t))^{\mathrm{T}}\cdot\mathbf{R}_{\mathbf{v}}(t)\cdot\Delta\mathbf{d}^{\mathrm{MS},t_0}} \\ & \times p_{\phi_{n,m}^{\mathrm{MS}}(t),\theta_{n,m}^{\mathrm{MS}}(t)}(\phi_n^{\mathrm{MS}}(t),\theta_n^{\mathrm{MS}}(t))\mathrm{d}\phi_n^{\mathrm{MS}}\mathrm{d}\theta_n^{\mathrm{MS}}\end{aligned} \tag{10}$$

where $\Delta\mathbf{d}^{\mathrm{BS}} = \mathbf{d}_{s_1}^{\mathrm{BS}} - \mathbf{d}_{s_2}^{\mathrm{BS}}$ denotes the space lag at the BS which does not change over time, $\Delta\mathbf{d}^{\mathrm{MS}}(t) = \mathbf{R}_{\mathbf{V}}(t) \cdot \Delta\mathbf{d}^{\mathrm{MS},t_0}$ denoted the time-variant space lag at the MS, and $\Delta\mathbf{d}^{\mathrm{MS},t_0} = \Delta\mathbf{d}_{u_1}^{\mathrm{MS},t_0} - \mathbf{d}_{u_2}^{\mathrm{MS},t_0}$ means the initial space lag. In (9) and (10), $p_{\phi_{n,m}^{\mathrm{BS/MS}}(t),\theta_{n,m}^{\mathrm{BS/MS}}(t)}(\phi_n^{\mathrm{BS/MS}}(t),\theta_n^{\mathrm{BS/MS}}(t))$ represents the time-variant joint probability density function

(PDF) of random angles, i.e., AAoDs $\phi_n^{\mathrm{BS}}(t)$ and EAoDs $\theta_n^{\mathrm{BS}}(t)$, or AAoAs $\phi_n^{\mathrm{MS}}(t)$ and EAoAs $\theta_n^{\mathrm{MS}}(t)$.

B. Approximate Expressions of SCFs

For several standard channel models, e.g., WINNER+ model and 3GPP-3D model, the azimuth and elevation angles of AoAs and AoDs are supposed to be independent and obey Gaussian and Laplacian distributions, respectively. However, Mammasis *et al.* [4] demonstrated that they are related under some scenarios and the flexible VMF distribution can fit measurement data better. The PDF of VMF distribution is defined as

$$p(\phi,\theta)=\frac{\kappa}{4\pi\sinh(\kappa)}\cos\theta \mathrm{e}^{\kappa\left(\cos\theta\cos\bar{\theta}\cos(\phi-\bar{\phi})+\sin\theta\sin\bar{\theta}\right)} \tag{11}$$

where $-\pi\le\phi\le\pi, -\pi/2\le\theta\le\pi/2$, $\bar{\phi}$ and $\bar{\theta}$ represent the mean values of azimuth and elevation angles, respectively, and κ controls the concentration of VMF distribution.

By substituting (11) into (9) and (10), the theoretical SCFs at the BS and MS under VMF scattering scenarios can be obtained. However, it is difficult to derive the accurate closed-form expressions of SCFs. In the following, we will derive the corresponding approximate expressions, which are very helpful to investigate the impact of 3D arbitrary trajectories on the SC. Let us take $\rho^{\mathrm{MS}}_{u_1,u_2,n}(t;\Delta\mathbf{d}^{\mathrm{MS}})$ as an example. By setting $\theta_n^{\mathrm{MS}}(t)=\bar{\theta}_n^{\mathrm{MS}}(t)+\zeta$ and $\phi_n^{\mathrm{MS}}(t)=\bar{\phi}_n^{\mathrm{MS}}(t)+\upsilon$ and substituting them into (10), it yields

$$\rho^{\mathrm{MS}}_{u_1,u_2,n}(t;\Delta\mathbf{d}^{\mathrm{MS}})=\int\limits_{\{\zeta,\upsilon\}}\int\frac{\kappa\cos(\bar{\theta}_n^{\mathrm{MS}}(t)+\zeta)A^{\mathrm{MS}}\ B^{\mathrm{MS}}}{4\pi\sinh(\kappa)}\mathrm{d}\zeta\mathrm{d}\upsilon \tag{12}$$

where

$$A^{\mathrm{MS}}=\mathrm{e}^{\kappa\left(\cos(\bar{\theta}_n^{\mathrm{MS}}(t)+\zeta)\cos\bar{\theta}_n^{\mathrm{MS}}(t)\cos(\upsilon)+\sin(\bar{\theta}_n^{\mathrm{MS}}(t)+\zeta)\sin\bar{\theta}_n^{\mathrm{MS}}(t)\right)} \tag{13a}$$

$$B^{\mathrm{MS}}=\mathrm{e}^{\mathrm{j}\mathrm{k}\tilde{\mathbf{s}}(\bar{\phi}_n^{\mathrm{MS}}(t)+\upsilon,\bar{\theta}_n^{\mathrm{MS}}(t)+\zeta)\mathbf{R}_{\mathbf{V}}(t)\Delta\mathbf{d}^{\mathrm{MS},t_0}}. \tag{13b}$$

The measured data has shown that the angle spreads are small under some scenarios, which means ζ and υ are small or the parameter κ is big [4]. Holding this condition, we have $\cos(\zeta)\approx\cos(\upsilon)\approx 1$, $\sin(\zeta)\approx\zeta$, $\sin(\upsilon)\approx\upsilon$, $\kappa\cos(\upsilon)\approx\kappa(1-\upsilon^2/2)$, and $\kappa\cos(\zeta)\approx\kappa(1-\zeta^2/2)$. By using the integration formula, we can obtain the approximate expression of (14) as

$$\begin{aligned}\rho^{\mathrm{MS}}_{u_1,u_2,n}(t;\Delta\mathbf{d}^{\mathrm{MS}})\approx&\frac{-\mathrm{Im}(\mathrm{erfi}(G^{\mathrm{MS}}(t)))\mathrm{Im}(\mathrm{erfi}(H^{\mathrm{MS}}(t)))}{8\sinh(\kappa)}\\&\times\mathrm{e}^{\mathrm{j}\mathrm{k}\tilde{\mathbf{s}}(\bar{\phi}_n^{\mathrm{MS}}(t),\bar{\theta}_n^{\mathrm{MS}}(t))\mathbf{R}_{\mathbf{V}}(t)\Delta\mathbf{d}^{\mathrm{MS},t_0}}\\&\times\mathrm{e}^{-(\mathrm{k}\mathbf{R}_{\mathbf{V}}(t)\Delta\mathbf{d}^{\mathrm{MS},t_0})^2((\frac{\mathbf{E}^{\mathrm{MS}}(t)}{\sqrt{2\kappa}})^2+(\frac{\mathbf{D}^{\mathrm{MS}}(t)}{\sqrt{2\kappa}})^2)+\kappa}.\end{aligned} \tag{14}$$

where erfi$(\cdot)$ is the imaginary error function,

$$\mathbf{D}^{\mathrm{MS}}(t)=[-\sin\bar{\theta}_n^{\mathrm{MS}}(t)\cos\bar{\phi}_n^{\mathrm{MS}}(t),-\sin\bar{\theta}_n^{\mathrm{MS}}(t)\sin\bar{\phi}_n^{\mathrm{MS}}(t),\cos\bar{\theta}_n^{\mathrm{MS}}(t)] \tag{15a}$$

$$\mathbf{E}^{\mathrm{MS}}(t)=[-\sin\bar{\phi}_n^{\mathrm{MS}}(t),\cos\bar{\phi}_n^{\mathrm{MS}}(t),0] \tag{15b}$$

$$G^{\mathrm{MS}}(t)=\frac{\mathrm{k}\mathbf{E}^{\mathrm{MS}}(t)\mathbf{R}_{\mathbf{V}}(t)\Delta\mathbf{d}^{\mathrm{MS},t_0}-\mathrm{j}\kappa\cos^2(\bar{\theta}_n^{\mathrm{MS}}(t))\Delta_\phi^{\mathrm{MS}}}{\sqrt{2\kappa\cos^2(\bar{\theta}_n^{\mathrm{MS}}(t))}} \tag{15c}$$

$$H^{\mathrm{MS}}(t)=\frac{\mathrm{k}\mathbf{D}^{\mathrm{MS}}(t)\mathbf{R}_{\mathbf{V}}(t)\Delta\mathbf{d}^{\mathrm{MS},t_0}-\mathrm{j}\kappa\Delta_\theta^{\mathrm{MS}}}{\sqrt{2\kappa}}. \tag{15d}$$

TABLE I
PARAMETERS OF THREE DIFFERENT TRAJECTORIES

Path	Valid	v_0 (m/s)	a (m/s^2)	ϕ_0	ω_ϕ (s^{-1})	θ_0	ω_θ (s^{-1})
I(1D linear)	①,②,③	10	0	0	0	0	0
II(2D curve)	②,③	10	0.065	$5\pi/36$	$-\pi/36$	0	0
III(3D arbitrary)	③	10	0.045	$\pi/12$	$-\pi/60$	$\pi/12$	$-\pi/60$

① the models in [5]–[8], ② the models in [9], [10], ③ the proposed model

In a similar way, we can derive the approximate expression of $\rho^{\mathrm{BS}}_{s_1,s_2,n}(t;\Delta\mathbf{d}^{\mathrm{BS}})$ as

$$\begin{aligned}\rho^{\mathrm{BS}}_{s_1,s_2,n}(t;\Delta\mathbf{d}^{\mathrm{BS}})\approx&\frac{-\mathrm{Im}(\mathrm{erfi}(G^{\mathrm{BS}}(t)))\mathrm{Im}(\mathrm{erfi}(H^{\mathrm{BS}}(t)))}{8\sinh(\kappa)}\\&\times\mathrm{e}^{\mathrm{j}\mathrm{k}\tilde{\mathbf{s}}(\bar{\phi}_n^{\mathrm{BS}}(t),\bar{\theta}_n^{\mathrm{BS}}(t))\Delta\mathbf{d}^{\mathrm{BS},t_0}-(\mathrm{k}\Delta\mathbf{d}^{\mathrm{BS},t_0})^2((\frac{\mathbf{E}^{\mathrm{BS}}(t)}{\sqrt{2\kappa}})^2+(\frac{\mathbf{D}^{\mathrm{BS}}(t)}{\sqrt{2\kappa}})^2)+\kappa}.\end{aligned} \tag{16}$$

where

$$\mathbf{D}^{\mathrm{BS}}(t)=[-\sin\bar{\theta}_n^{\mathrm{BS}}(t)\cos\bar{\phi}_n^{\mathrm{BS}}(t),-\sin\bar{\theta}_n^{\mathrm{BS}}(t)\sin\bar{\phi}_n^{\mathrm{BS}}(t),\cos\bar{\theta}_n^{\mathrm{BS}}(t)] \tag{17a}$$

$$\mathbf{E}^{\mathrm{BS}}(t)=[-\sin\bar{\phi}_n^{\mathrm{BS}}(t),\cos\bar{\phi}_n^{\mathrm{BS}}(t),0] \tag{17b}$$

$$G^{\mathrm{BS}}(t)=\frac{\mathrm{k}\mathbf{E}^{\mathrm{BS}}(t)\Delta\mathbf{d}^{\mathrm{BS},t_0}-\mathrm{j}\kappa\cos^2(\bar{\theta}_n^{\mathrm{BS}}(t))\Delta_\phi^{\mathrm{BS}}}{\sqrt{2\kappa\cos^2(\bar{\theta}_n^{\mathrm{BS}}(t))}} \tag{17c}$$

$$H^{\mathrm{BS}}(t)=\frac{\mathrm{k}\mathbf{D}^{\mathrm{BS}}(t)\Delta\mathbf{d}^{\mathrm{BS},t_0}-\mathrm{j}\kappa\Delta_\theta^{\mathrm{BS}}}{\sqrt{2\kappa}}. \tag{17d}$$

Finally, combining (8) and (14)–(17), the approximate SCF of the proposed generic 3D non-stationary GBSM can be obtained.

IV. SIMULATION RESULTS AND ANALYSIS

In the simulation, the time-variant speed and direction models in [13] are adopted, i.e., $v^{\mathrm{MS}}(t)=v_0+a\cdot t$, $\phi_{\mathbf{V}}(t)=\phi_0+\omega_\phi\cdot t$, and $\theta_{\mathbf{V}}(t)=\theta_0+\omega_\theta\cdot t$, where v_0 is the initial speed, a is the acceleration of speed, ϕ_0 and θ_0 are the initial azimuth and elevation of movement, respectively, ω_ϕ and ω_θ are the corresponding angular speeds. To verify the effectiveness of proposed generic GBSM and the derived theoretical SCF, three kinds of trajectories with the same start point and end point, i.e., 1D linear trajectory, 2D curve trajectory, and 3D arbitrary trajectory, were selected and rest simulation parameters are summarized in Table I. Note that our proposed model are suitable for all three paths, while the models in [8]–[10] chosen to compare only support Path I or Path II as shown in Table I.

According to the definition of (9) and (10), the absolute values of theoretical SCFs of our generic 3D non-stationary GBSM for Paths I–III at $t=4$ s are shown in Fig. 1. For comparison purpose, the SCFs of 3D non-stationary GBSMs in [8]–[10] for Path I or Path II at $t=4$ s are also given. It can be observed that the SCFs of our model agree well with the one in [8] for Path I, and the ones in [9] and [10] for Path II, which means the proposed generic GBSM is compatible with existing ones under 1D and 2D trajectories. In addition, it also shows that different trajectories have a great impact on the correlation properties of channel models.

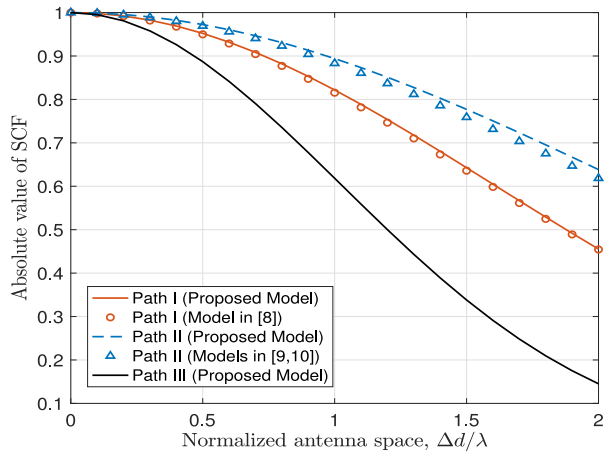

Fig. 1. Absolute values of the theoretical SCFs of our proposed model and other models for three paths at $t = 4$ s (UMi NLOS scenario, $\kappa = 65$, v^{A_n} and $v^{\mathrm{Z}_n}\sim$U(0,5) m/s, ϕ^{A_n} and $\phi^{\mathrm{Z}_n}\sim\mathrm{U}(-\pi,\pi)$, θ^{A_n} and $\theta^{\mathrm{Z}_n}\sim\mathrm{U}(-\pi/2,\pi/2)$).

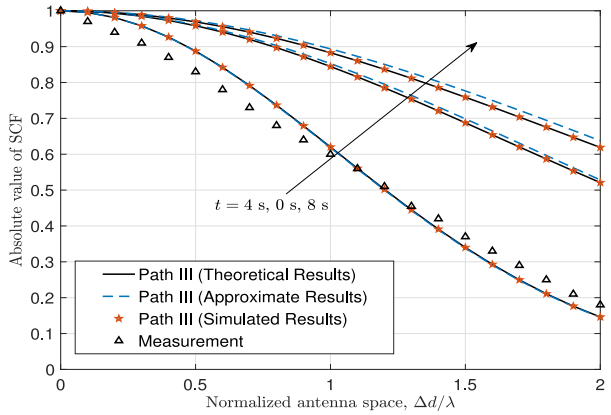

Fig. 2. Absolute values of the theoretical, approximated, simulated SCFs of the proposed model for Path III at three time instants and the measured SCF in [14] (UMi NLOS scenario, $\kappa = 65$, v^{A_n} and $v^{\mathrm{Z}_n}\sim$U(0,5) m/s, ϕ^{A_n} and $\phi^{\mathrm{Z}_n}\sim\mathrm{U}(-\pi,\pi)$, θ^{A_n} and $\theta^{\mathrm{Z}_n}\sim\mathrm{U}(-\pi/2,\pi/2)$).

The theoretical results of SCFs at $t = 0$ s, 4 s, and 8 s of proposed GBSM for path III are compared with the simulated and approximate results in Fig. 2. It clearly shows that SCFs change over time due to the movement of the MS. Meanwhile, the measurement results in [14] are also shown in Fig. 2. The good agreement between measured, theoretical, approximate, and simulated SCFs shows the correctness of both the proposed model and theoretical derivations.

V. Conclusion

We have proposed a generic 3D non-stationary GBSM incorporating 3D arbitrary trajectories and 3D antenna arrays of the MS in this letter. The proposed model is compatible with the existing 3D non-stationary GBSMs for 1D and 2D trajectories. In addition, the corresponding theoretical and approximate expressions of SCFs under VMF scattering scenarios have also been derived and verified by simulations and measurements. These results can significantly improve the efficiency of analyzing the SC and performance of MIMO communication systems. In the future, we will further analyze other time-varying statistical properties of this proposed GBSM, i.e., the autocorrelation function (ACF) and Doppler power spectrum density (DPSD), and investigate the impact of different trajectories on the system performance.

References

[1] C.-X. Wang *et al.*, "Recent advances and future challenges for massive MIMO channel measurements and models," *Sci. China Inf. Sci.*, vol. 59, no. 2, pp. 1–16, Feb. 2016.

[2] J.-A. Tsai, R. M. Buehrer, and B. D. Woerner, "BER performance of a uniform circular array versus a uniform linear array in a mobile radio environment," *IEEE Trans. Wireless Commun.*, vol. 3, no. 3, pp. 695–700, May 2004.

[3] Q.-U.-A. Nadeem, A. Kammoun, M. Debbah, and M.-S. Alouini, "A generalized spatial correlation model for 3D MIMO channels based on the Fourier coefficients of power spectrums," *IEEE Trans. Signal Process.*, vol. 63, no. 14, pp. 3671–3686, Jul. 2015.

[4] K. Mammasis, R. W. Stewart, and J. S. Thompson, "Spatial fading correlation model using mixtures of Von Mises Fisher distributions," *IEEE Trans. Wireless Commun.*, vol. 8, no. 4, pp. 2046–2055, Apr. 2009.

[5] J. Bian *et al.*, "A WINNER+ based 3-D non-stationary wideband MIMO channel model," *IEEE Trans. Wireless Commun.*, vol. 17, no. 3, pp. 1755–1767, Mar. 2018.

[6] S. Wu, C.-X. Wang, M. Aggoune, M. M. Alwakeel, and X. You, "A general 3D non-stationary 5G wireless channel model," *IEEE Trans. Commun.*, vol. 66, no. 7, pp. 3065–3078, Jul. 2018.

[7] A. G. Zajić, "Impact of moving scatterers on vehicle-to-vehicle narrowband channel characteristics," *IEEE Trans. Veh. Technol.*, vol. 63, no. 7, pp. 3094–3106, Sep. 2014.

[8] Q. Zhu *et al.*, "A novel 3D non-stationary wireless MIMO channel simulator and hardware emulator," *IEEE Trans. Commun.*, vol. 66, no. 9, pp. 3865–3878, Sep. 2018.

[9] J. Bian, C.-X. Wang, M. Zhang, X. Ge, and X. Gao, "A 3-D non-stationary wideband MIMO channel model allowing for velocity variations of the mobile station," in *Proc. ICC*, Paris, France, Jul. 2017, pp. 1–6.

[10] A. Borhani, G. L. Stüber, and M. Pätzold, "A random trajectory approach for the development of nonstationary channel models capturing different scales of fading," *IEEE Trans. Veh. Technol.*, vol. 66, no. 1, pp. 2–14, Jan. 2017.

[11] H. Hofstertter, A. F. Molisch, and N. Czink, "A twin-cluster MIMO channel model," in *Proc. EuCAP*, Nice, France, Nov. 2006, pp. 1–8.

[12] B. Boashash. *Time-Frequency Signal Analysis and Processing: A Comprehensive Reference*. Amsterdam, The Netherlands: Academic, 2015.

[13] W. Dahech, M. Pätzold, C. A. Gutiérrez, and N. Youssef, "A non-stationary mobile-to-mobile channel model allowing for velocity and trajectory variations of the mobile stations," *IEEE Trans. Wireless Commun.*, vol. 16, no. 3, pp. 1987–2000, Mar. 2017.

[14] S. Payami and F. Tufvesson, "Channel measurements and analysis for very large array systems at 2.6 GHz," in *Proc. Antennas Propag. (EUCAP)*, Prague, Czech Republic, Mar. 2012, pp. 433–437.